archives
of thermodynamics
Vol. **38**(2017), No. 1, 27–38
DOI: 10.1515/aoter-2017-0002

Thermodynamic study of phase equilibrium of superionic alloys of $Ag_3SBr_{1-x}Cl_x$ system in the concentration range 0.0–0.4 and temperature range 370–395 K

M.V. MOROZ[a*]
M.V. PROKHORENKO[b]
S.V. PROKHORENKO[c]
O.V. RESHETNYAK[d]

[a] Department of Chemistry and Physics, National University of Water and Environmental Engineering, Soborna 11, 33028 Rivne, Ukraine

[b] Department of Cartography and Geospatial Modeling, Lviv Polytechnic National University, St. Bandery 12, 79013 Lviv, Ukraine

[c] Center for Microelectronics and Nanotechnology, University of Rzeszow, Pigonia 1, 35959 Rzeszow, Poland

[d] Department of Physical and Colloid Chemistry, Ivan Franko National University of Lviv, Kyryla i Mefodiya 6, 79005 Lviv, Ukraine

Abstract Thermodynamic assessment of the phase stability of the solid solutions of superionic alloys of the $Ag_3SBr_{1-x}Cl_x$ (I) system in the concentration range $0 \leq x \leq 0.4$ and temperature range 370–395 K was performed. Partial functions of silver in the alloys of solid solution were used as the thermodynamic parameters. The values of partial thermodynamic functions were obtained with the use of the electromotive force method. Potential-forming processes were performed in electrochemical cells. Linear dependence of the electromotive force of cells on temperature was used to calculate the partial thermodynamic functions of silver in the alloys. The serpentine-like shape of the thermodynamic functions in the concentration range 0–4 is an evidence of the metastable state of solid solution. The equilibrium phase state of the alloys is predicted to feature the formation of

*Corresponding Author. E-mail: riv018@i.ua

the intermediate phase $Ag_3SBr_{0.76}Cl_{0.24}$, and the solubility gap of the solid solution ranges of $Ag_3SBr_{0.76}Cl_{0.24}$ and Ag_3SBr.

Keywords: Phase equilibrium; Superionic alloys; Thermodynamic properties; Gibbs energy; EMF method

Nomenclature

DTA	–	differential thermal analysis
ECC	–	electrochemical cell
EMF	–	electromotive force
PSD	–	position sensitive detector
XRD	–	X-ray difraction
E	–	EMF, V
T	–	temperature, K
$T_{ph.t}$	–	phase transition temperature
G	–	Gibbs energy, kJ mol^{-1}
H	–	enthalpy, kJ mol^{-1}
p	–	pressure, Pa
S	–	entropy, J (mol K)$^{-1}$
x	–	concentration
$\Delta\overline{G}^{\circ}_{298}$	–	partial Gibbs energy of silver in alloys of solid solution of $Ag_3SBr_{1-x}Cl_x$ system at T=298 K, kJ mol^{-1}
$\Delta_r G_T$	–	Gibbs energy of reaction, kJ mol^{-1}

Greek symbols

α, β, γ	–	modifications of phases
ρ	–	density, kg m^{-3}
θ	–	angle, degree

1 Introduction

The Ag_3SI and Ag_3SBr compounds are characterized by polymorphism γ–$Ag_3SI \xrightarrow{159\,K} \beta$–$Ag_3SI \xrightarrow{508\,K} \alpha$–$Ag_3SI$, γ–$Ag_3SBr \xrightarrow{128\,K} \beta$–$Ag_3SBr$, as well as the superionic state of β-phases at room temperature. The formation of solid solutions $Ag_3SI_{1-x}Br_x$ $(0 \le x \le 1)$ and $Ag_3SBr_{1-x}Cl_x$ $(0 \le x \le 0.4)$ [1–6], where x – concentraction of halogen in $Ag_3SBR_{1-x}Cl_x$ alloys, was found with the participation of ternary compounds. The substitution Br→I in the solid electrolyte Ag_3SBr is accompanied by the increase of ionic conductivity and by the decrease of the temperature of the phase transition to the superionic state $\gamma \longrightarrow \beta$ [4]. In the case of Br→Cl substitution the temperature of phase transition to the superionic state increases. The temperature dependences of conductivity for the four-element alloys above

the phase transition temperature are little different [6]. Such properties are due to the inclusions of free molecular groups Ag_2S in the alloys. The integral thermodynamic properties of Ag_3SI and Ag_3SBr compounds were calculated in [7, 8].

An important part for the practical application of the superionic alloys is their state of thermodynamic equilibrium. The accurate information on the equilibrium or metastable state of compounds and solid solutions can be obtained by the use of the electromotive force (EMF) method [9]. For instance, partial thermodynamic functions of silver in the alloys of continuous solid solution series Ag_8GeS_6-Ag_8SnS_6 were determined in [10] using the EMF method in the range of 300–390 K. The monotonous course of the concentration changes of the functions indicates the equilibrium state of the continuous solid solution series at room temperature.

This paper presents the results of experiments and calculations of the values of partial thermodynamic functions $\Delta\overline{G}^{\circ}_{298}$, $\Delta\overline{H}^{\circ}_{298}$, and $\Delta_r\overline{S}^{\circ}_{298}$ of silver in the alloys of the $Ag_3SBr_{1-x}Cl_x$ (I) system, to obtain data on the thermodynamic equilibrium or metastable state of the single-phase alloys in a concentration range $0 \leq x \leq 0.4$ and temperature range 370–395 K. The analysis of the concentration changes of the functions was performed by the concepts of physicochemical analysis, namely principles of continuity and correspondence [11].

2 Experimental

The crystalline and glassy alloys were prepared from the components and compounds of high purity (Tab. 1). Alloys of the $Ag_3SBr_{1-x}Cl_x$ system were obtained from the well-mixed powder blend (particle size $\leq 5\,\mu$m) of AgBr, AgCl compounds and Ag, S elements. Molar fraction of sulfur in the mixture exceeded the calculated value by about 5%. The crystalline Ag, Ge, S and AgBr were used for the synthesis of Ag_3GeS_3Br glass. The components were placed into quartz ampoules and evacuated to the residual pressure ~1 Pa. Alloys of the system (I) ($0 \leq x \leq 0.4$) were obtained by heating the ampoules to 1073 K, isothermal annealing for about 2 h followed by cooling to room temperature [6]. Crystals were ground into powder to the particle size of less then 5 μm and homogenized by annealing in vacuum (pressures about 1 Pa) at 600 K for 48 h. Free sulfur was removed by vacuum distillation at 380 K. These alloys were then used in differential thermal analysis (DTA) and X-ray diffraction (XRD) methods,

and employed as positive electrodes of electrochemical cells (ECCs). Glass was obtained by melt quenching from 1200 K into ice water.

Table 1: Provenance and purities of the materials used in this study.

Chemical name	Manufacturer	Country of manufacture and city	Mass fraction of purity
Ag (powder)	Alfa Aesar	Germany, Karlsruhe	0.9995
S	Lenreactiv	Russia, Saint-Petersburg	0.9999
Ge	Lenreactiv	Russia, Saint-Petersburg	0.9999
AgBr	Lenreactiv	Russia, Saint-Petersburg	0.9980
AgCl	Lenreactiv	Russia, Saint-Petersburg	0.9980
H_2	Lviv chemical factory	Ukraine, Lviv	0.9990
Ar	Lviv chemical factory	Ukraine, Lviv	0.9990

The phase composition of the alloys was monitored by DTA and XRD methods. The DTA curves of alloys were recorded using a Paulik-Paulik-Erdey derivatograph fitted with chromel-alumel thermocouples and H307-1 XY recorder. The thermocouples were calibrated by the melting points of In (429 K), Sn (505 K), Cd (594 K), Te (723 K), Sb (904 K), NaCl (1074 K), Ge (1209 K), Ag (1236 K), Cu (1357 K) [12]. The heating (cooling) rate of the alloys in the DTA scans was 6–8 K min^{-1}, and the temperature measurement error did not exceed ±5 K. X-ray powder diffraction patterns were collected using the automated Stoe Stadi P diffractometer equipped with a source of Cu K α_1 radiation (monochromatized with curved germanium [1 1 1] crystal) and a linear position sensitive detector (PSD), transmission sample holder, generator 40 kV and 40 mA. The calibration procedure was performed utilizing NIST SRM 640b (Si) [13] and NIST SRM 676 (Al_2O_3) [14] standards. The diffraction measurements were performed in transmission mode within the 5.000°–100.505° 2-range with a 2θ step of 0.015° with the following settings: PSD step 0.480° 2θ, measurement time 100 s/step, where θ is the diffracted angle. Preliminary data processing, and phase analysis from XRD patterns were performed using the Stoe WinXpow (version 2.21) program package [15] and PowderCell (version 2.3) [16].

Potential-forming processes were performed in ECCs of the type

(–)C | Ag | Ag_3GeS_3Br glass | D | C (+) where C are the inert graphite electrodes; Ag and D are the electrodes of ECCs; D represents the alloys (I) of the $0 \leq x \leq 0.4$ range; and Ag_3GeS_3Br glass is a membrane with purely ionic Ag^+ conductivity [17]. Glassy Ag_3GeS_3Br, like Ag_3GeS_3I [18], belongs to the class of superionic materials [19]. The equilibrium state in ECCs (E = const) was achieved in time not exceeding 2–4 h. The equilibrium was considered when the EMF values were constant or their variations did not exceed ± 0.2 mV for 30 min.

Powdered cell components were pressed ($p \sim 10^8$ Pa) into through holes with the diameter of 2 mm arranged in the polytetrafluoroethylene (PTFE) matrix up to the density $\rho = (0.93 \pm 0.02)\rho_0$, where ρ_0 is the experimentally determined density of cast alloys. To eliminate the defects of plastic deformation under extrusion of alloys, we performed thermal cycling of ECCs twice in the range of 350–400 K with heating and cooling rates of 2 K min^{-1} [17, 20]. The ECCs were heated in a resistance furnace similar to that described in [21] filled with a mixture of H_2 and Ar in a molar ratio of 1:9, $p = 1.2 \times 10^5$ Pa. The flow of gas at the rate of 2×10^{-3} m^3h^{-1} had a direction from the positive to the negative electrode of the ECC. The temperature was maintained with an accuracy of ±0.5 K. The EMF values of the cells were measured using the voltmeter of a U7–9 electrometric amplifier with an input resistance of greater then 10^{12} Ω. The temperature dependences of the EMF of the cells, $E(T)$, were analyzed according to technique described in [22,23].

3 Results and discussion

Gibbs tetrahedron of the Ag-S-Br-Cl system is shown in Fig. 1. Two-phase equilibria lines mark out four-phase regions: AgCl-Ag_2S-Ag_3SBr-Ag (II), AgCl-Ag_2S-Ag_3SBr-S (III), Ag-Ag_3SBr-AgCl-AgBr, and Ag_3SBr–S-AgCl-AgBr. The Ag_3SBr-"Ag_3SCl" section determines the positions of the figurative points of the alloys of $Ag_3SBr_{1-x}Cl_x$ solid solution in the AgCl–Ag_2S–Ag_3SBr region which is common for regions (II) and (III).

Silver-rich alloys (I) of the phase region (II) are unsuitable for the use as positive electrodes of ECCs because of the phase equilibrium with silver metal. The stoichiometric alloy of Ag_3SBr is difficult to obtain [3,6]. Polycrystalline samples synthesized by solid-phase reaction methods, crystallization from the melt, precipitation from aqueous solution were not stoichiometric. XRD and calorimetric investigations always show uncontrolled

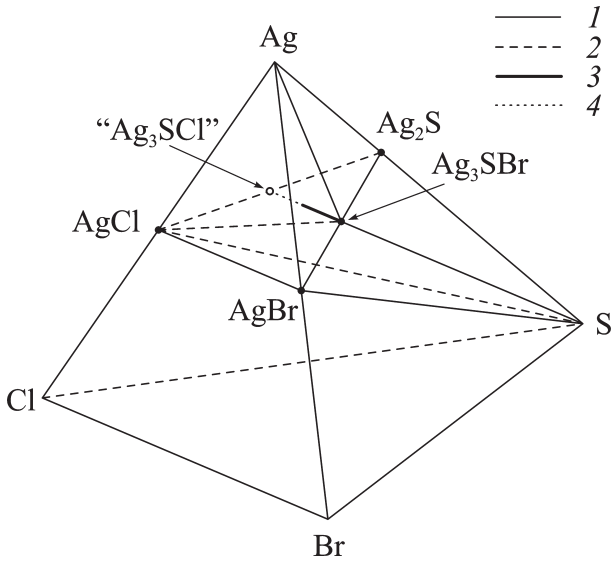

Figure 1: Triangulation of the Ag-S-Br-Cl system in the concentration region Ag-S-AgBr-AgCl at $T < 600$ K: quasi-quaternary systems AgCl-Ag_2S-Ag_3SBr-Ag, AgCl-Ag_2S-Ag_3SBr-S, Ag-Ag_3SBr-AgCl-AgBr and Ag_3SBr-S-AgCl-AgBr; *1*, *2* are lines of two-phase equilibria; *3*, *4* are single-phase and three-phase regions of the Ag_3SBr – "Ag_3SCl" section.

quantity of unreacted AgBr. It is noted that the deviation from stoichiometry does not cause significant changes in temperature of the phase transition but the value of ionic conductivity in superionic phase is very sensitive to the unreacted amount of silver bromide. Therefore, we used alloys (I) of the phase region (III), i.e., in equilibrium with sulfur, as the positive electrodes D of ECCs.

Some typical dependences of ECCs, E, on temperature, T, in the range of 360–410 K are shown in Fig. 2. The deviations of $E(T)$ from the linearity below 370 K is due to the kinetic hindrances to the completion of uncontrolled reactions $Ag^+ + e^- \longrightarrow Ag + D$ in alloys D [24]. These reactions result in the shift of the figurative point of D in Gibbs tetrahedron to the point of silver. Halide anions in D (bromide and chloride) at $T \geq 395$ K acquire likely the properties of mobile quasi-liquid [17]. In this case the positive electrode is characterized by a nonuniform distribution of the electrical charge along the ECC axis. The negative charge of mobile Br^-, Cl^- is localized in the narrow region of the interface Ag_3GeS_3Br glass D, whereas the excess positive charge is distributed within the rest of D. Under

these conditions the nonlinearity of $E(T)$ is the result of the variation of nonuniform distribution of charge in D with temperature.

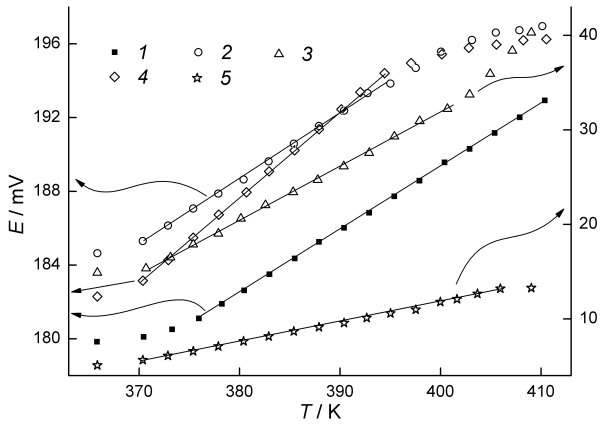

Figure 2: Dependences of EMF, E, vs. temperature, T, of electrochemical cells: *1–5* correspond to alloys of the phase compositions $x = 0$, 0.15, 0.25, 0.30, and 0.40 respectively.

Linear dependences of EMF, E, on temperature, T, of the cells in nine alloys of $Ag_3SBr_{1-x}Cl_x$ system in the 370–395 K range were calculated by the least squares method and are expressed by the following relations (E in millivolts, mV; T in Kelvin, K plus dimensionless quantity):

$$E_{x=0} = (52.24093 \pm 0.43012) + (0.34272 \pm 0.00109)T \ , \tag{1}$$

$$E_{x=0.05} = (77.64582 \pm 0.85126) + (0.29961 \pm 0.00214)T \ , \tag{2}$$

$$E_{x=0.10} = (75.47235 \pm 0.98121) + (0.30269 \pm 0.00255)T \ , \tag{3}$$

$$E_{x=0.15} = (50.90435 \pm 1.21169) + (0.36253 \pm 0.00315)T \ , \tag{4}$$

$$E_{x=0.20} = (-37.73872 \pm 0.2519) + (0.47299 \pm 0.00406)T \ , \tag{5}$$

$$E_{x=0.25} = (-196.79017 \pm 1.84081) + (0.57165 \pm 0.00476)T \ , \tag{6}$$

$$E_{x=0.30} = (11.69254 \pm 1.56252) + (0.46336 \pm 0.00408)T \ , \tag{7}$$

$$E_{x=0.35} = (-25.5692 \pm 0.87142) + (0.32271 \pm 0.00713)T \ , \tag{8}$$

$$E_{x=0.40} = (-67.96458 \pm 0.47669) + (0.19869 \pm 0.00123)T \ . \tag{9}$$

From the measured $E(T)$ relations, Gibbs energies were calculated using the basic thermodynamic equation

$$-\Delta_r G_T = n\mathrm{F}E \ , \tag{10}$$

where $n = 1$ is the valence of the potential-forming ion (Ag^+), and F = 96485.3 C mol $^{-1}$ is the Faraday number.

The following equations were obtained from (1)–(10), ($\Delta_r G$ in kJ mol $^{-1}$; T in Kelvin, K plus dimensionless quantity):

$$\Delta_r G_{T,x=0} = (-5.04 \pm 0.04) - (33.07 \pm 0.11) \times 10^{-3} T \ , \tag{11}$$

$$\Delta_r G_{T,x=0.05} = (-7.49 \pm 0.09) - (28.91 \pm 0.21) \times 10^{-3} T \ , \tag{12}$$

$$\Delta_r G_{T,x=0.10} = (-7.29 \pm 0.10) - (29.21 \pm 0.25) \times 10^{-3} T \ , \tag{13}$$

$$\Delta_r G_{T,x=0.15} = (-4.91 \pm 0.12) - (34.71 \pm 0.31) \times 10^{-3} T \ , \tag{14}$$

$$\Delta_r G_{T,x=0.20} = (3.64 \pm 0.31) - (45.64 \pm 0.39) \times 10^{-3} T \ , \tag{15}$$

$$\Delta_r G_{T,x=0.25} = (18.99 \pm 0.18) - (55.16 \pm 0.46) \times 10^{-3} T \ , \tag{16}$$

$$\Delta_r G_{T,x=0.30} = (-1.13 \pm 0.15) - (44.71 \pm 0.40) \times 10^{-3} T \ , \tag{17}$$

$$\Delta_r G_{T,x=0.35} = (2.47 \pm 0.09 - (31.13 \pm 0.69) \times 10^{-3} T \ , \tag{18}$$

$$\Delta_r G_{T,x=0.40} = (6.56 \pm 0.05) - (19.17 \pm 0.12) \times 10^{-3} T \ . \tag{19}$$

Equations (11)–(19) express the temperature dependence of the partial Gibbs energy of silver in alloys $Ag_3SBr_{1-x}Cl_x$. The values of partial thermodynamic functions of silver in the solid solution alloys calculated from Eq. (11)–(19) in approximation $\left(\frac{\partial \Delta_r H}{\partial T}\right)_p = \left(\frac{\partial \Delta_r S}{\partial T}\right)_p = 0$ are listed in Tab. 2 and their concentration changes are shown in Fig. 3. Table 2 includes $T\Delta_r S$ products to compare the contribution from structural and energy $\Delta_r H$ parameters to $\Delta_r G$ value.

The serpentine-like shape of the concentration changes of the partial thermodynamic functions is an evidence of the metastable state of $Ag_3SBr_{1-x}Cl_x$ solid solution in the temperature range 370–395 K. The thermodynamic conditions of the decomposition of the solid solution (I) appear at phase transition temperature, $T_{ph.tr}$, in the subsolidus range. The crystal structure of the alloys (I) is such that the vibrational energy of the atoms (groups of atoms) is insufficient for the emergence of a new phase. Below $T_{ph.tr.}$ alloys (I) are metastable. The maxima of the concentration changes of the functions in the vicinity of the $Ag_3SBr_{0.76}Cl_{0.24}$

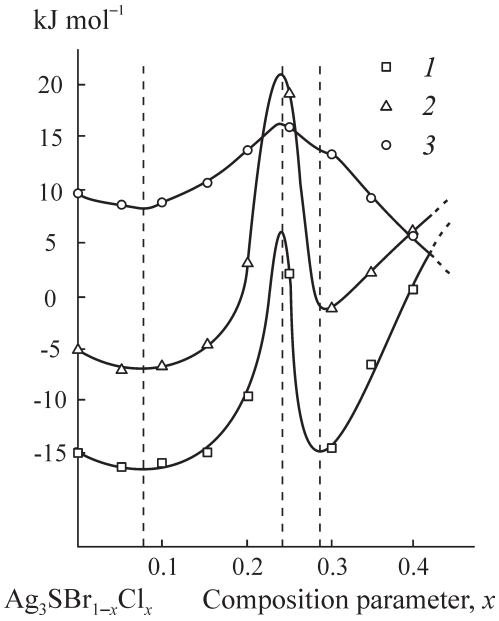

Figure 3: Concentration changes of partial thermodynamic functions of silver in alloys of the solid solution of $Ag_3SBr_{1-x}Cl_x$ system in the range of 370–395 K: *1* – $\Delta\overline{G}^{\circ}_{298}$, *2* –$\Delta\overline{H}^{\circ}_{298}$, *3* – $T\Delta_r\overline{S}^{\circ}_{298}$.

Table 2: Partial thermodynamic functions of silver in superionic alloys of $Ag_3SBr_{1-x}Cl_x$ $(0 \leq x \leq 0.4)$ system in standard state.

Concentration of halogen x in $Ag_3SBr_{1-x}Cl_x$ alloys	$\Delta\overline{G}^{\circ}_{298}$, kJ mol $^{-1}$	$\Delta\overline{H}^{\circ}_{298}$, kJ mol $^{-1}$	$\Delta_r\overline{S}^{\circ}_{298}$, J (mol E) $^{-1}$	$T\Delta_r\overline{S}^{\circ}_{298}$, kJ mol $^{-1}$
0.00	–14.89 ± 0.06	–5.04 ± 0.04	33.07 ± 0.11	9.85 ± 0.04
0.05	–16.10 ± 0.11	–7.49 ± 0.09	28.91 ± 0.21	8.61 ± 0.06
0.10	–15.99 ± 0.12	–7.29 ± 0.10	29.21 ± 0.25	8.70 ± 0.08
0.15	–15.25 ± 0.16	–4.91 ± 0.12	34.71 ± 0.31	10.34 ± 0.10
0.20	–9.96 ± 0.13	3.64 ± 0.31	45.64 ± 0.39	13.60 ± 0.12
0.25	2.55 ± 0.12	18.99 ± 0.18	55.16 ± 0.46	16.44 ± 0.14
0.30	–14.45 ± 0.20	–1.13 ± 0.15	44.71 ± 0.40	13.32 ± 0.12
0.35	–6.81 ± 0.22	2.47 ± 0.09	31.13 ± 0.69	9.28 ± 0.21
0.40	0.85 ± 0.07	6.56 ± 0.05	19.17 ± 0.12	5.71 ± 0.04

alloy indicate the existence, upon reaching the equilibrium state of (I), of the intermediate phase of this composition. The equilibrium phase diagram (I) in the $Ag_3SBr_{0.76}Cl_{0.24}$–Ag_3SBr section would feature a solubility gap of the solid solution ranges. The monotonous flow of the concentration changes of $\Delta\overline{G}^{\circ}_{298}$, $\Delta\overline{H}^{\circ}_{298}$ and $T\Delta_r\overline{S}^{\circ}_{298}$ for $x > 0.3$ indicates the existence in the system (I) in equilibrium state of another one intermediate phase in the range of 0.4–1.0. The minima on the curves at $x = 0.075$ and $x = 0.28$ are due to the limited solid solubility based on the four-element phase.

4 Conclusions

The serpentine-like shape of the concentration changes of the partial thermodynamic functions of silver in the superionic alloys of the $Ag_3SBr_{1-x}Cl_x$ system (T = 370–395 K) indicates the state of solid solution in the concentration range $0 \leq x \leq 0.4$ as metastable. Upon achieving the equilibrium state of the $Ag_3SBr_{1-x}Cl_x$ system, the formation of the intermediate phase $Ag_3SBr_{0.76}Cl_{0.24}$ and the solubility gap in the concentration range Ag_3SBr–$Ag_3SBr_{0.76}Cl_{0.24}$ are predicted. The equilibrium state of the alloys is characterized by an intermediate phase $Ag_3SBr_{0.76}Cl_{0.24}$. Solid solution ranges of Ag_3SBr and $Ag_3SBr_{0.76}Cl_{0.24}$ of the equilibrium system $Ag_3SBr_{1-x}Cl_x$ are separated by a two-phase region. The monotonous flow of the changes with concentration for $x > 0.3$ indicates the existence in the equilibrium system $Ag_3SBr_{1-x}Cl_x$ of another intermediate phase in the range of $0.4 \leq x \leq 1.0$.

Received September 2016

References

[1] Hoshino S., Fujishita H., Takashige M., Sakuma T.: *Phase transition of Ag_3SX (X = I, Br)*. Solid State Ionics **3-4**(1981), 35–39, DOI:10.1016/0167-2738(81)90050-3.

[2] Kettai M.El., Malugani J.P., Mercier R., Tachez M.: *Phase transitions and conductivity in superionic $Ag_3SI_{1-x}Br_x$ solid solutions.* Solid State Ionics **20**(1986), 87–92, DOI:10.1016/0167-2738(86)90014-7.

[3] Beeken R.B., Haase A.T., Hoerman B.H., Klawikowski S.J.: *The effect of non-stoichometry in Ag_3SBr.* Solid State Ionics **113-115**(1998), 509–513, DOI:10.1016/S0167-2738(98)00384-1.

[4] Beeken R.B., Menningen K.L.: *Fast ion conduction in β-$Ag_3SI_{1-x}Br_x$ solid solutions.* J. Appl. Phys. **66**(1989), 11, 5340–5343, http://dx.doi.org/10.1063/1.343726.

[5] Xianglian, Honda H., Basar K., Siagian S., Sakuma T., Takahashi H., Kawaji H., Atake T.: *Low-Temperature Phase in Superionic Conductor $Ag_3SBr_xI_{1-x}$*. J. Phys. Soc. Jpn. **76**(2007), 114603, 1–4, http://dx.doi.org/10.1143/JPSJ.76.114603.

[6] Beeken R.B., Wright T.J., Sakuma T.: *Effect of chloride substitution in the fast ion conductor Ag_3SBr*. J. Appl. Phys. **85**(1999), 11, 7635–7638, http://dx.doi.org/10.1063/1.370565.

[7] Babanly M.B., Mashadieva L.F., Velieva G.M., Imamalieva S.Z., Shykhyev Yu.M.: *Thermodynamic study of the Ag-As-Se and Ag-S-I systems using the EMF method with a solid Ag_4RbI_5 electrolyte*. Russ. J. Electrochem. **45**(2009), 4, 399–404, DOI:10.1134/S1023193509040077.

[8] Moroz M.V., Prokhorenko M.V., Prokhorenko S.V.: *Determination of thermodynamic properties of Ag_3SBr superionic phase using EMF technique*. Russ. J. Electrochem. **51**(2015), 886–889, DOI:10.1134/S1023193515090098.

[9] Babanly M., Yusibov Y., Babanly N.: *The EMF Method with Solid-State Electrolyte in the Thermodynamic Investigation of Ternary Copper and Silver Chalcogenides*. In: Electromotive Force and Measurement in Several Systems, (S. Kara, Ed.), InTech, 2011.

[10] Aliyeva Z.M., Bagheri S.M., Aliev Z.S., Alverdiyev I.J., Yusibov Y.A., Babanly M.B.: *The phase equilibria in the Ag_2S–Ag_8GeS_6–Ag_8SnS_6 system*. J. Alloys Compd. **611**(2014), 395–400, doi:10.1016/j.jallcom.2014.05.112.

[11] Fairman R., Ushkov B. (Eds.): *Semiconducting Chalcogenide Glass I: Glass Formation, Structure, and Simulated Transformations in Chalcogenide Glasses*, Vol. 78, Elsevier – Academic Press, 2004.

[12] Preston-Thomas H.: *The international temperature scale of 1990 (ITS-90)*. Metrologia. **27**(1990), 1, 3–10.

[13] *SRM 640b: Silicon Powder 2θ/d-Spacing Standard for X-ray Diffraction*. National Institute of Standards and Technology, Gaithersburg, MD, 1987.

[14] *Standard Reference Materials, SRM 676: Alumina Internal Standard for Quantitative Analysis by X-ray Powder Diffraction*. National Institute of Standards and Technology, Gaithersburg, MD, 2005.

[15] *Diffractometer Stoe WinX^{POW}*, version 2.21, Stoe & Cie GmbH, Darmstadt 2007.

[16] Kraus W., Nolze G.: *PowderCell for Windows, version 2.3*. Federal Institute for Materials Research and Testing, Berlin 1999.

[17] Moroz M.V., Demchenko P.Yu., Prokhorenko S.V., Moroz V.M.: *Physical properties of glasses in the Ag_2GeS_3-AgBr system*. Phys. Solid State. **55**(2013), 8, 1613–1618, DOI: 10.1134/S1063783413080209.

[18] Robinel E., Kone A., Duclot M.J., Souquet J.L.: *Silver sulfide based glasses:(II). Electrochemical properties of GeS_2-Ag_2S-AgI glasses: Transference number measurement and redox stability range*. J. Non-Cryst. Solids **57**(1983), 1, 59–70, DOI: 10.1016/0022-3093(83)90408-8.

[19] West A.R.: *Solid State Chemistry and its Application*, 2nd Edn. Wiley, 2014.

[20] Moroz M.V., Demchenko P.Yu., Mykolaychuk O.G., Akselrud L.G., Gladyshevskii R.E.: *Synthesis and electrical conductivity of crystalline and glassy alloys in the Ag_3GeS_3Br–GeS_2 system.* Inorg. Mater. **49**(2013), 9, 867–871, DOI:10.1134/S0020168513090100.

[21] Feng D., Taskinen P., Tasfaye F.: *Thermodynamic stability of Ag_2Se from 350 to 500 K by a solid state galvanic cell.* Solid State Ionics. **231**(2013), 1–4, DOI:10.1016/j.ssi.2012.10.013.

[22] Osadchii E.G., Echmaeva E.A.: *The system Ag–Au–Se: Phase relations below 405 K and determination of standard thermodynamic properties of selenides by solid-state galvanic cell technique.* Am. Mineral. **92**(2007), 4, 640–647, DOI:10.2138/am.2007.2209

[23] Moroz M.V., Prokhorenko M.V.: *Thermodynamic properties of the intermediante phases of the Ag–Sb–Se system.* Russ. J. Phys. Chem. A. **88**(2014), 5, 742–746, DOI:10.1134/S0036024414050203.

[24] Morachevskiy A.G., Voronin G.F., Geyderikh V.A., Kutsenyuk I.B.: *Electrochemical Methods of Investigation in Thermodynamics of Metallic Systems.*Akademkniga, Moscow 2003 (in Russian).